PSpice modelling of the Pulsed Electro Acoustic device: A new approach to account attenuation, dispersion and reflection phenomena

A. Pujol, Fulbert Baudoin, Laurent Berquez, Denis Payan

PSpice modelling of the Pulsed Electro Acoustic device: A new approach to account attenuation, dispersion and reflection phenomena

A. Pujol (1), F. Baudoin (1), L. Berquez (1), D. Payan (2)
(1) Laboratoire plasma et conversion d'énergie, 118 route de Narbonne, 31062, Toulouse, France
(2) Centre national d'études spatiales, 18 avenue Edouard Belin, 31401, Toulouse, France

***Abstract*- The Pulsed Electro Acoustic (PEA) method is very common to study the transport of space charges inside dielectric. Unfortunately, the current calibration of the transfer matrix does not take into account some phenomenon as reflections, attenuation and dispersion of the pressure wave going through the sample. Analytical models of the PEA help to bring this lack of information to the matrix transfer. In this study, we first introduce an electrical PSpice model, based on analytical ones, to define a new transfer matrix of the PEA. Second, we present a new method for the deconvolution of an experimental PEA signal.**

I. Introduction

Many satellite's mission difficulties are due to space charge occurrences as dielectric breakdown [1]. One useful system for space charge measurement is the Pulsed Electro Acoustic (PEA) introduced by Takada [2]. This method is non-destructive and its aim is to stimulate charges by an electrical pulse and measuring the acoustic response with a piezoelectric transducer. A mathematical processing is applied on the output voltage of the sensor to recover the charges distribution inside the dielectric sample. This processing is first based on a calibration step to define the PEA transfer function. So far, the calibration is made with an output signal generated from an input well-known Dirac capacitive charge at the interface between the sample and the ground electrode[3]. Unfortunately, the transfer function resulting from this procedure does not take into account the dispersive propagation of the acoustic wave inside the sample. The acoustic distortion due to the wave generation near the High-Voltage (HV) electrode or inside thin sample (under $50\,\mu m$) are not considered too. First, an improved PSpice model based on [1] including acoustic waves attenuation and dispersion is presented. Second, this model is used to build a PEA transfer matrix. Finally, this matrix is employed to deconvoluate the experimental signal by using an improved regularization method based on the Tikhonov [4] one.

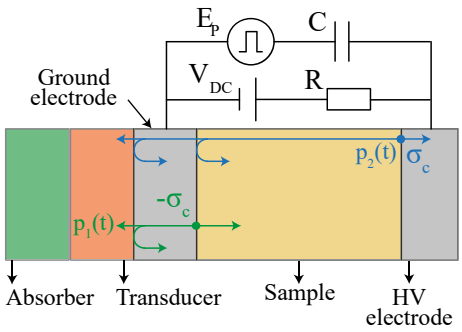

Fig. 1. PEA in biasing configuration

II. PSpice model of the PEA

A. Overview

The PEA device is shown in the Fig. 1 under biasing configuration. A brief description is given here, for further details refer to [5]–[7]. A DC voltage generator V_{DC} produces opposite sheet capacitive charges $\pm\sigma_c$ at each electrode. A pulsed electric field E_p is employed to stress the charges. For a dielectric sample that is no polar, no piezoelectric and no electrostrictive [5], p_1 is the pressure force generated by the convolution between the pulsed electric field and the capacitive charges $-\sigma_c$ at the ground electrode, and p_2 is the one created at the HV electrode. Fig. 1 only shows the reflections of the pressure forces that affect the useful signal. A part of both pressure waves propagates to the transducer that convert these acoustic waves to an electrical signal. Finally, this signal is amplified to be measured. Note that both dipoles R and C are used to decouple V_{DC} and E_P.

The PEA system can be modeled by a PSpice electrical network as shown in the Fig. 2. Both pressure forces are modeled by voltage generators and all acoustic media by transmission lines, respecting the acoustic-electric analogy. The transducer is made up by the Redwood's Model [6]. The

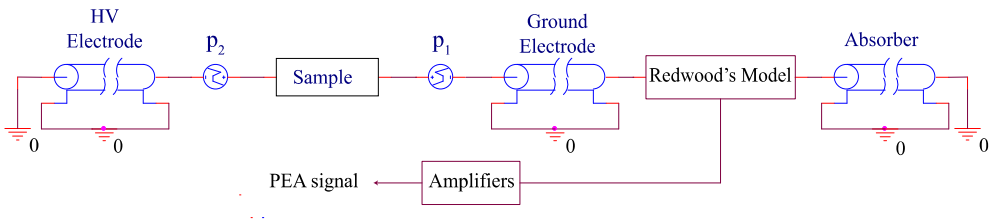

Fig. 2. PSpice model of the PEA

amplifiers are defined by two 27 dB gains and a 50 Ω input resistance.

Equations (1)-(4) reveal how to set transmission line parameters from acoustic medium values [7]. L is the linear inductance that represents the linear mass of the medium which depends on the density ρ and the surface S. The linear capacitance C_p describes the medium's elasticity which is proportional to the acoustic velocity c_{ac}. The linear resistance R defines the friction losses which is related to the viscous losses α. The linear conductance G illustrates the thermal losses which are negligible, for the different media, compared to the viscous losses.

$$L = \rho S \quad (1)$$

$$C_p = \frac{1}{\rho S {c_{ac}}^2} \quad (2)$$

$$R = 2\rho S\alpha \quad (3)$$

$$G = 0 \quad (4)$$

These relations are correct for low losses, which means for a given pulsation ω, $R \ll L\omega$ and $G \ll C_p\omega$.

Except the sample, all acoustic media are modeled by an ideal transmission line using (1)-(2). Because the dielectric sample attenuates and disperses the acoustic wave, (3) and (2) need to be modified to consider frequency dependent losses and velocity.

B. Model of lossy and dispersive polymeric sample

The losses and the velocity can depend on the frequency for some dielectrics and be measured from an experimental signal of the PEA in its biasing configuration. The Fig. 3 shows both voltage peaks V_1 and V_2 engendered by both pressure forces p_1 and p_2 previously seen.

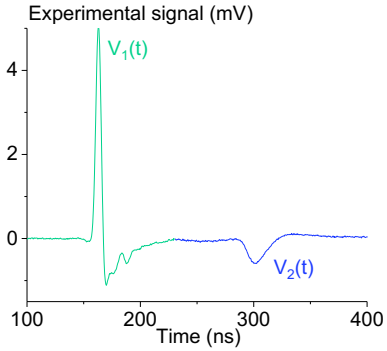

Fig. 3. Experimental signal

Respecting that the frequency response of the transducer is constant in the frequency range of interest, then its transient output voltage is proportional to its input pressure force. This leads to the next frequency relations:

$$FFT(V_1) = KG_{S\to G}.FFT(p_1) \quad (5)$$

$$FFT(V_2) = KG_{HV\to S}T_{S\to G}e^{-\left[\alpha(f)+\frac{j2\pi f}{c_{ac}(f)}\right]l}FFT(p_2) \quad (6)$$

K is a factor modeling the response of the transducer and l is the length of the sample. The exponential term represents the attenuation and the dispersion of the pressure force p_2 to the transducer. $G_{S\to G}$ and $G_{HV\to S}$ are respectively the generation coefficients at the ground and the HV electrode interfaces. $T_{S\to G}$ is the transmission coefficient at the ground electrode interface. They are defined by:

$$G_{S\to G} = \frac{Z_G}{Z_S+Z_G} \quad (7)$$

$$G_{HV\to S} = \frac{Z_S}{Z_{HV}+Z_S} \quad (8)$$

$$T_{S\to G} = \frac{2Z_G}{Z_S+Z_G} \quad (9)$$

Z_G, Z_S and Z_{HV} are respectively the mechanical impedance of the ground electrode, the sample and the HV electrode. Ditchi et al [8] suggested in 1993 a process to determine the losses and the velocity factors of an insulating material without the generation effect at the HV interface. We propose a method to take into account this mismatching impedance effect using (8) and (9):

$$\alpha(f) - \frac{1}{l}ln(2G_{HV\to S}) = -\frac{1}{l}ln\left|\frac{FFT(-V_2)}{FFT(V_1)}\right| \quad (10)$$

$$c_{ac}(f) = \frac{-2\pi fl}{\varphi(FFT(-V_2))-\varphi(FFT(V_1))} \quad (11)$$

The plots of these experimental coefficients are shown in the Fig. 4. These factors have to be modeled by functions to be substituted in (3) and (2). Polynomial regressions can be achieved but the losses and velocity values for low frequency are inaccurate because of the use of FFT modulus and phase in the denominators. It is why the following model is often employed.

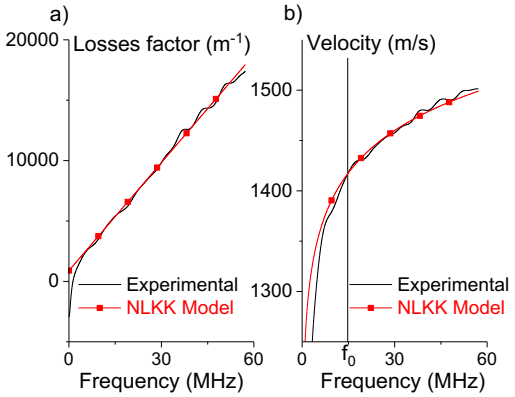

Fig. 4. a) Losses factor, b) Velocity

Older studies show that the viscous losses of a polymeric material can be linear to the frequency f.

$$\alpha(f) - a_0 = af \quad (12)$$

To respect the causality of the material, the Nearly Local Kramers-Kroning (NLKK) relation links $\alpha(f)$ and $c_{ac}(f)$:

$$c_{ac}(f) = c_{ac}(f_0) + \left(\frac{c_{ac}(f_0)}{\pi}\right)^2 a.ln\left(\frac{f}{f_0}\right) \quad (13)$$

This relation is acceptable for materials having no sharp resonance in the frequency range of interest $|c_{ac}(f) - c_{ac}(f_0)| \ll c_{ac}(f_0)$, and if:

$$\left[\frac{\alpha(f)c_{ac}(f)}{2\pi f}\right]^2 \ll 1 \quad (14)$$

Fig. 4 shows the fitting of (10) and (11) to (12) and (13) in order to determine the NLKK parameters. The practicable bandwidth of this PEA signal is 60 MHZ. The values obtain from the NLKK regression are:

$$Z_{HV} = 294\ N.s/m$$
$$a = 298\ (m.MHz)^{-1}$$
$$f_0 = 14.8\ MHz$$
$$c_{ac}(f_0) = 1417\ m/s$$

$\alpha(f)$ and $c_{ac}(f)$ in (10) and (11) are then substituted in (3) and (2) to define a Frequency Dependent Transmission Line (FDTL). Unfortunately, the PSpice lossy transmission line component cannot consider any frequency dependent values in passive elements such as the capacitance. This line is then insert into PSpice using the Method of Characteristics (MoC) of Brainin [9].

The modelling of the lossy and dispersive polymeric sample leads to compare the PSpice simulation of the PEA to the experimental signal.

C. *Simulation versus experiment*

The experiment was operated under biasing configuration as seen in the Fig. 1. The DC voltage has been setup to 1 kV. The electrical pulse width is 3 ns and its amplitude is 300 V.

The physical values used to set the model are presented in the TABLE I. The Levenberg-Marquardt [10] algorithm has been employed to optimize some of these values in order to fit better the experimental signal. These parameters have been modified within an interval close to literature values.

TABLE I

	HV Electrode	Sample	Ground Electrode	Acoustic transducer	Absorber
Materials	LDPE	PTFE	Aluminum	PVDF	PMMA
Length (μm)	1000	205	10000	10.9	2000
Density (g/cm^3)	1410	2200	2700	1524	1132
Speed of sound (m/s)	2200	1350	6400	2250	2750
Relative permittivity				7	
Dielectric loss angle				0.02	

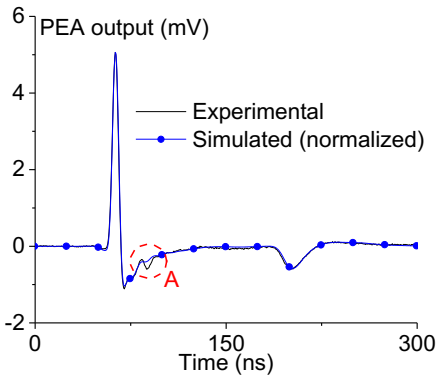

Fig. 5. PEA output signal

The comparison between the simulation and the experimental signal is presented in the Fig. 5. The relative error is only 7.6 %. It shows up the efficiency of the model to fit the experiment. However, the model cannot fit well inside the A area. This part of the experimental signal is probably due to the electrical pulse form.

Note that:

- A Gaussian filter has been applied to the simulated signal. Indeed, our model bandwidth is larger than the experimental one maybe because the aluminum ground electrode dispersion is not considered.
- The simulated signal amplitude has been normalized to the experimental one that is four time lower. This is probably because the ground electrode losses are not considered.

This adjusted model can help to define the PEA transfer matrix.

III. Signal Processing of the PEA

A. *PEA transfer matrix determination*

The PEA system is built from the PSpice model (cf. Fig. 2). An input pressure force is defined as the convolution between the capacitive charge and the pulsed electric field. The sample is discretized under layers for which the length is Δx. A simulation loop is made to set the pressure force input p_i into different layer for each iteration. Every simulation provides a PEA response h_{PEA} with a temporal sampling T_s. The matrix transfer is then built step by step a shown in the Fig. 6.

Note that the following condition, between the space sampling of the sample Δx and the temporal sampling of the PEA signal T_s, is necessary to respect CFL and avoid any numerical diffusion:

$$\Delta x \geq \max\left(c_{ac}(f)\right)T_s \qquad (15)$$

This matrix has a high condition number that leads to a large number of solutions by reversing the matrix to find the charge distribution. Method of regularization have to be used to obtain a noiseless deconvolution of the measurement signal.

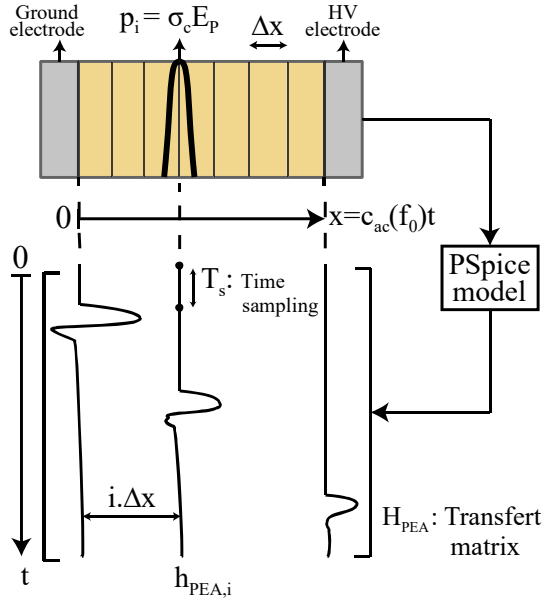

Fig. 6. PEA transfer matrix building

B. *Deconvolution processing of the PEA measurement*

One method of regularization largely used is the Tikhonov one. This deconvolution does not recover a Dirac charge σ but it provides a volume distribution of the charge ρ respecting:

$$\int \rho(x)dx = \sigma(x) \tag{16}$$

The Tikhonov method consists to minimize the residual norm and the solution norm:

$$\|h_{PEA}.\rho - V_{PEA}\|_2^2 + \lambda\|\Gamma\rho\|_2^2 \tag{17}$$

Γ is the Tikhonov matrix that should be chosen according to the problem. In this study, Γ is set to the identity matrix I in order to give preference to solution with smaller norm. λ is the regularization parameter. It controls the balance between both norms of (17) to provide the optimal solution:

$$\rho_{opt} = \frac{{h_{PEA}}^T V_{PEA}}{{h_{PEA}}^T h_{PEA} + \lambda_{opt} I} \tag{18}$$

The optimal regularization parameter λ_{opt} is defined by using the L-curve method [11]. Equation (18) provides an analytical solution that is quickly calculated. This is the main advantage of Tikhonov method. However, minimizing the solution norm for this study is not the best choice. In fact, following this method provides a linear offset to the electric field due to an offset on the charge distribution obtained. A better choice for this problem is to minimize the average value of the solution in addition to the residual norm.

$$\|h_{PEA}.\rho - V_{PEA}\|_2^2 + \bar{\rho} \tag{19}$$

Indeed, the sum of the charges inside the dielectric sample is null because of the electrostatic equilibrium. It makes more sense to minimize a well-known equation than minimizing the solution. Unfortunately, there is no analytical solution of the optimal charges distribution as for the Tikhonov method. The minimization of (19) is realized by an iterative numerical method using the Levenberg-Marquardt [10] algorithm. With any knowledge on the charge distribution, the iterative loop starts with a zero vector solution and then converge to the final solution. It takes more time to obtain the charges distribution compared to the Tikhonov method but the linear offset of the electric field disappeared. In this study, a hybrid deconvolution has been done. First, the Tikhonov regularization has been applied to obtain a charges distribution vector including an offset. Second, this vector is used to start the minimization loop of (19). The number of iterations spend 10 to 1.

Fig. 7 shows the solution of the distribution charges and the electric field obtained by the signal processing introduced in this study and an older signal processing that does not consider the generation and the propagation of the pressure wave through the sample. The charge distribution at the ground electrode obtained by the older method has a better space resolution than the one presented in this investigation. However, the charge distribution at the HV electrode has a better resolution for the presented method and it leads to an electric field that respect electrostatic equilibrium.

IV. Conclusion

A PSpice model of the PEA has been presented in this study. It helps to build a transfer matrix of the PEA that takes into account the generation and the propagation of the pressure force for different space positions inside the sample. An investigational testing has been done on a $205\,\mu m$ PTFE sample that is a material attenuating and diffusing pressure wave. This test has been conclusive and it will be an interesting thing to test multi-layers and thin dielectric sample.

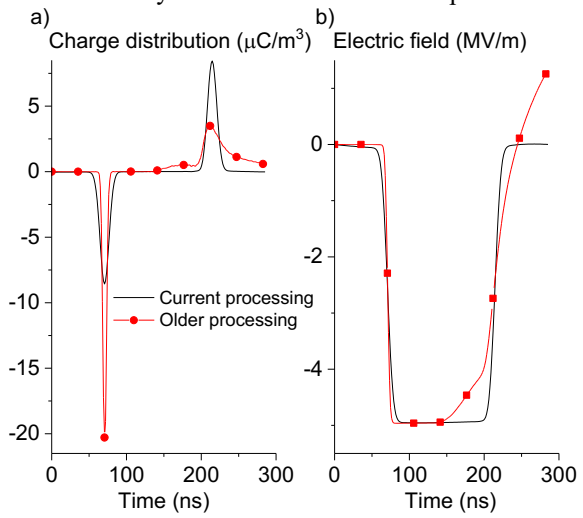

Fig. 7. a) Charge distribution, b) Electric field

References

[1] L. Galloy, L. Berquez, F. Baudoin, and D. Payan, "PSpice modeling of the pulsed electro-acoustic signal," *IEEE Trans. Dielectr. Electr. Insul.*, vol. 21, no. 3, pp. 1143–1153, Jun. 2014.

[2] T. Takada, T. Maeno, and H. Kushibe, "An Electric Stress-Pulse Technique for The Measurement of Charges in A Plastic Plate Irradiated by an Electron Beam," *IEEE Trans. Electr. Insul.*, vol. EI-22, no. 4, pp. 497–501, Aug. 1987.

[3] T. Maeno, T. Futami, H. Kushibe, T. Takada, and C. M. Cooke, "Measurement of spatial charge distribution in thick dielectrics using the pulsed electroacoustic method," *IEEE Trans. Electr. Insul.*, vol. 23, no. 3, pp. 433–439, Jun. 1988.

[4] R. A. Willoughby, "Solutions of Ill-Posed Problems (A. N. Tikhonov and V. Y. Arsenin)," *SIAM Rev.*, vol. 21, no. 2, pp. 266–267, Apr. 1979.

[5] S. Holé, T. Ditchi, and J. Lewiner, "Influence of divergent electric fields on space-charge distribution measurements by elastic methods," *Phys. Rev. B*, vol. 61, no. 20, pp. 13528–13539, May 2000.

[6] M. Redwood, "Transient Performance of a Piezoelectric Transducer," *J. Acoust. Soc. Am.*, vol. 33, no. 4, pp. 527–536, Apr. 1961.

[7] J. van Deventer, T. Lofqvist, and J. Delsing, "PSpice simulation of ultrasonic systems," *IEEE Trans. Ultrason. Ferroelectr. Freq. Control*, vol. 47, pp. 1014–24, Feb. 2000.

[8] T. Ditchi, C. Alquié, and J. Lewiner, "Broadband determination of ultrasonic attenuation and phase velocity in insulating materials," *J. Acoust. Soc. Am.*, vol. 94, no. 6, pp. 3061–3066, Dec. 1993.

[9] F. H. Branin, "Transient analysis of lossless transmission lines," *Proc. IEEE*, vol. 55, no. 11, pp. 2012–2013, Nov. 1967.

[10] D. W. Marquardt, "An Algorithm for Least-Squares Estimation of Nonlinear Parameters," *J. Soc. Ind. Appl. Math.*, vol. 11, no. 2, pp. 431–441, 1963.

[11] P. Christian. Hansen and D. Prost. O'Leary, "The Use of the L-Curve in the Regularization of Discrete Ill-Posed Problems," *SIAM J. Sci. Comput.*, vol. 14, no. 6, pp. 1487–1503, Nov. 1993.